

The Memory Effect in Electron Glasses

Eran Lebanon and Markus Müller

*Center for Materials Theory, Serin Physics Laboratory, Rutgers University,
136 Frelinghuysen Road, Piscataway, New Jersey 08854-8019, USA*

We present a theory for the memory effect in electron glasses. It is manifested in fast gate voltage sweeps as a dip in the conductivity around the equilibration gate voltage. We show that this feature, also known as the anomalous field effect, arises from the long-time persistence of correlations in the electronic configuration. We argue that the gate voltage at which the memory dip saturates is determined by the instability of the glassy state upon the injection of a critical number of excess carriers. We find that this saturation gate voltage increases with temperature, whereas the gate voltage beyond which memory erasure occurs is temperature independent. Using standard percolation arguments, we calculate the anomalous field effect as a function of gate voltage, temperature, carrier density and disorder. Our results are consistent with experiments, and in particular, they reproduce the observed scaling of the width of the memory dip with various parameters.

PACS numbers: 73.61.Jc

I. INTRODUCTION

The unscreened Coulomb interactions between localized electrons in dirty semiconductors or granular metallic films lead to glassy behavior such as slow relaxation, history dependence of observables, non-ergodicity, and memory effects. Even though such Coulomb glasses were theoretically predicted more than twenty years ago^{1,2,3,4}, it was a major task to provide convincing experimental evidence for their existence. To our knowledge, very slow electronic relaxation was first reported in the context of capacitance measurements in doped GaAs by Monroe et al.⁵. At temperatures well below 1K, they observed relaxation times that reached the scale of tens of seconds. Even more striking non-equilibrium behavior was found by Ovadyahu's group in the conductivity of strongly disordered indium-oxide films⁶, where the logarithmic relaxation can extend up to several hours (a typical experimental set-up is shown in Fig. 1). Over the last decade, very careful and systematic studies of this system have demonstrated that the electronic out-of-equilibrium behavior is indeed due to the strong frustration induced by the Coulomb interactions between localized electrons, and does not primarily reflect the glassy dynamics of extrinsic degrees of freedom⁷. All the key features usually associated with a glassy system have been observed in this system: Aging, i.e., the increase of a characteristic relaxation time with the time the system has had to explore phase space^{8,9}, the dependence of sample properties on its history^{10,11} and memory effects¹². The latter appear as a dip in the film conductivity as the gate voltage is swept through the point at which the system was equilibrated for a long time. The memory of these equilibration conditions usually persists for several hours after the gate voltage has been changed to a new value.

A very similar anomalous field effect, accompanied by slow relaxation, was observed in various granular metals such as Au¹³, Al¹⁴, as well as Bi and Pb^{15,16}. Furthermore, the aging behavior and the temperature dependence of the memory dip reported in granular Al¹⁷ are

very similar to those found in indium-oxide films¹⁸. This suggests that these glassy effects are rather universal, even though the details of the hopping mechanism and the temperature dependence of the resistivity are clearly different in the two systems.

It has long been conjectured that the glassy memory dip reflects to some extent the Coulomb gap in the density of states^{19,20} which originates from the unscreened Coulomb interactions, too. This conjecture has been bolstered by recent theoretical works that show that the emergence and the universality of the Coulomb gap are closely related to a glass transition at a finite T_g in these systems^{21,22}.

The perspective of obtaining information on Coulomb correlations is a very appealing aspect of the memory experiments. For a long time experimental evidence for the Coulomb gap in doped semiconductors was only indirect in the form of the Efros-Shklovskii hopping law $R(T) \sim \exp[(T_{ES}/T)^{1/2}]$, see, e.g.,²³ for a review. In the last ten years, several tunneling experiments on weakly insulating samples exhibited a clear pseudogap around the Fermi level^{24,25,26,27,28}. However, most of these experiments are restricted to the regime relatively close to the metal-insulator transition. The memory effect thus provides a rather unique method to probe Coulomb correlations also further in the insulating regime. Furthermore, a closer analysis of the tunneling experiments and comparison with corresponding conductivity data reveal several discrepancies with the standard Efros-Shklovskii theory. Additional experimental information on Coulomb correlations from independent methods is therefore highly desirable.

The precise connection between the memory effect in Coulomb glasses and Efros-Shklovskii-type correlations in the electronic configuration has remained unclear so far. The aim of this paper is to review the experiments and theory for such systems (Sections II-V), and to analyze subsequently (Sections VI-VII) how the non-ergodicity of the glass state gives rise to the memory effect. We start with a detailed discussion of the glassy fea-

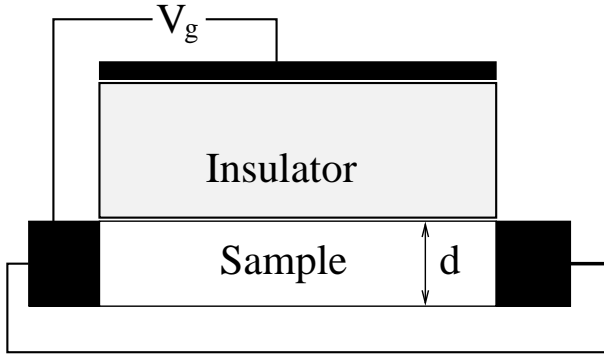


FIG. 1: Typical experimental setup: The sample is a film (semiconductor or granular metal) of thickness d , which is coupled capacitively to a gate electrode, kept at a bias V_g . The gate allows to vary slightly the number of carriers in the film. The conductivity of the sample is probed through contact electrodes that are directly attached to the sample.

tures observed in experiments in Section II, emphasizing the memory effect. In section III, we review the standard Efros-Shklovskii model for strongly localized electrons and discuss its applicability to systems with higher carrier density. In section IV, we review the theoretical results on the glass transition and its connection with the emergence of a Coulomb gap in the density of states. Section V recalls the percolation theory of hopping transport and discuss the dimensional crossover from bulk samples (3D) to films (2D) as a function of sample thickness. In section VI we develop a quantitative theory and confront the results with experiments. The approximations underlying our theory are discussed in section VII, and several open issues are addressed, too. Finally, we discuss the conditions under which glassiness can be observed in conductivity, and we conclude with a brief summary of our main results.

II. GLASSY BEHAVIOR IN EXPERIMENTS

A. Slow relaxation and aging

In this section, we discuss some of the experiments exhibiting glassy behavior. Monroe et al⁵ observed slow electronic relaxation upon the gate-controlled charge injection into p-type doped partially compensated GaAs with dopant density $n_A \approx 10^{17} \text{ cm}^{-3}$. The typical Coulomb energy in this system, $e^2 n_A^{1/3} / \kappa$, is of the order of 100 K and according to theoretical estimates (see Eq. (14) below), one may expect a glass transition at a temperature of the order of 3-4 K.

The authors monitored the penetration depth ΔL over which a small number of injected charges was distributed as a function of time. They found that the system equilibrated very rapidly for temperatures above 2 K while for lower temperatures ΔL relaxed only very slowly. Furthermore, the initial value of ΔL increased as the den-

sity of excess charges Δn decreased. This peculiar effect is due to non-linear screening²⁹ in a glassy system of localized electrons: The newly introduced carriers try to screen the weak gate field by occupying empty sites close to the gate, while minimizing their mutual repulsive interaction at the same time. This competition results in a charge distribution pattern of width $\Delta L \sim (\Delta n)^{-1/2}$, which can be much larger than the Thomas-Fermi-screening length $l_{TF} \sim (\nu_0 e^2 / \kappa)^{-1/2}$ that one might naively expect. Only after considerable collective rearrangements of the whole electron configuration, the charge distribution can actually relax to its ground state in which the excess charge will indeed be localized within l_{TF} from the surface²⁹. This non-linear screening effect also plays an important role in the memory effect in indium-oxide films, as we will discuss later.

More recently, very slow logarithmic relaxation was observed in the conductivity of various granular metals^{14,15,16}, as well as in indium-oxide films⁷. Furthermore, after equilibration under fixed experimental conditions and subsequent moderate excitation during a time t_w (e.g., by gate voltage⁷ or electric field⁹), the typical relaxation time of the system scales with t_w , a phenomenon known as simple aging. It is observed in many glassy systems such as polymers, spin glasses or supercooled liquids, and reflects the fact that the system remembers the time during which it has been perturbed. Simple aging comes about rather naturally if one supposes that, once taken out of its equilibrium state, the system explores phase space overcoming higher and higher barriers that are associated with increasingly long time scales. The local valley in energy landscape that the system reaches after a perturbation time t_w then typically has an escape time which is of the order of t_w , too.³⁰ With the assumption of a wide and rather featureless distribution of thermal or tunneling barriers, one can readily explain the logarithmic behavior of the relaxation³¹.

We believe that the barriers invoked in this picture should be associated with rather complicated many electron rearrangements, which are probably not related to the “slow” formation of the single particle Coulomb gap³². The latter should occur within a Maxwell time (proportional to the resistivity) which is still microscopic even for highly resistive samples. The numerical study of Ref.³³ indeed suggests that aging and slow relaxation is rather associated with inter-state transitions and a slow descent in the glassy energy landscape. Since at low temperatures all metastable states exhibit a kind of Coulomb gap suppression, the descent in the energy landscape will at best be reflected in some widening of the single particle gap and probably in more subtle electronic correlations that may affect the quasiparticle excitations that control the conductivity.

B. The memory effect

One of the most striking manifestations of the electron glass is the anomalous field effect: After the equilibration of the sample at some gate voltage V_g^0 , the subsequently measured traces of conductivity as a function of gate voltage will keep a long-lasting memory of these equilibrium conditions in the form of a symmetric dip around V_g^0 . The fact that the conductivity increases no matter whether carriers are added or depleted, can be understood on a qualitative level by the observation⁶ that any perturbation taking the system out of equilibrium must lead to an increase of the conductivity. On a more quantitative level one should explain the following experimental observations obtained from extensive studies on indium-oxide films (see Ref.¹⁰ for a comprehensive summary): The width and even the normalized shape of the memory dip, i.e., the conductivity measured as a function of gate voltage (or more precisely, as a function of density of induced excess carriers) is remarkably universal, even though its global amplitude may change by several orders of magnitude. More precisely, the width Γ of the dip is independent on the sweep rate or the application of a magnetic field. Even more surprisingly, it remains unchanged under thermal annealing, a process which reduces the disorder significantly and thus increases the conductivity by several orders of magnitude. However, the width Γ increases with carrier density, which is a strong indication for the relevance of electron-electron interactions⁷. Furthermore Γ increases roughly linearly with temperature, and keeps a certain memory of temperature: After a sudden quench from the equilibration temperature T to a lower temperature $T' < T$, the width Γ relaxes only slowly to the value corresponding to T' , keeping a memory of the larger width characteristic of T . Similar results, in particular the decrease of Γ with temperature and memory of higher temperatures, were recently found in granular aluminium films, too^{14,17}.

It is to be expected that memory effects and simple aging will break down once the sample is perturbed too strongly. This was indeed confirmed experimentally by applying large gate voltages¹¹ or in-plane electric fields⁹, as well as by illumination of the sample with energetic photons³⁴. One might expect that the gate voltage induced breakdown occurs at a constant multiple of the width Γ of the memory dip. However, it is found that the ratio of the two voltage scales increases with carrier density¹¹, indicating that the saturation of the dip and the erasure of memory are associated with two different energy scales.

C. Relaxation time

One can define a relaxation time in electron glasses as the time it takes to “heal” a memory dip at the gate voltage V_g^0 where the system was equilibrated and to create a dip at a new gate voltage³¹. In high density indium-

oxide films ($n_c > 5 \cdot 10^{20} \text{ cm}^{-3}$ this time is typically of the order of a few hundred seconds exhibiting no systematic dependence on carrier density. However, the relaxation time drops to unmeasurably small values once the carrier density is decreased below $n_{cr} \approx 10^{19} \text{ cm}^{-3}$, while the temperature is held constant at $T_m = 4 \text{ K}$ ¹². It is natural to suspect that this dramatic drop indicates the crossing of the glass transition line in the (T, n_c) -plane, as we will discuss in more detail in section IV.

So far a coherent picture that accounts for all these experimental observations was missing. Concerning the memory effect, we will show in Section VI that the key features of the memory dip can be understood at least semi-quantitatively from relatively simple arguments about the glassy free energy landscape and the stability of its local valleys.

III. LIMIT OF STRONGLY LOCALIZED ELECTRONS

A. Semiconductors with strongly localized electrons

In the literature, two standard models for semiconductors with localized electrons have been considered, see Refs.^{35,36} for a good review. The “classical impurity band” model refers to lightly doped, partially compensated semiconductors where all carriers are localized within a Bohr radius around majority impurities. (The term “energy strip” would probably be more appropriate than “band”.) Due to the Coulomb interactions with randomly distributed charged impurities, the on-site energies ϵ_i of these localized states are scattered over a range of the order of a few times the nearest neighbor interactions,

$$\sqrt{\overline{\epsilon_i^2}} \sim \frac{e^2}{\kappa r_c} \quad (1)$$

where $r_c \equiv n_c^{-1/3}$ is the average distance between carriers, n_c is the carrier density (uncompensated dopant concentration) and κ is the host dielectric constant. The overline denotes average over disorder. Accordingly, the bare density of localized states (neglecting Coulomb interactions between the localized carriers) is of the order of

$$\nu_0 = \frac{n_c}{e^2/\kappa r_c} = \frac{\kappa}{e^2} n_c^{2/3}, \quad (\text{impurity band}). \quad (2)$$

The second frequently considered model describes amorphous semiconductors in which the disorder of the on-site energies ϵ_i is due to strong local inhomogeneities. In this case their scatter is usually much larger than that introduced by Coulomb interactions with impurities, and as a consequence, the bare density of states is lower than (2), as schematically illustrated in Fig. 2.

In general, the set of localized states does not need to fill the whole pseudogap between the valence and the conduction band. In the case of indium-oxide (both amorphous³⁷ and crystalline³⁸), it has been established that the localized states form a tail joining the conduction band at the mobility edge. Furthermore, it was found that at sufficiently high carrier densities, the density of states in the range of localized states is in surprisingly good agreement with free-electron estimates,

$$\nu_0 \approx \frac{n_c}{\hbar^2 n_c^{2/3} / 2m}, \quad (\text{high density, } n_c > n_X) \quad (3)$$

reflecting the fact that the kinetic energy $E_{\text{kin}} = \hbar^2 k_F^2 / 2m$ of the localized wavefunctions dominates over the effects of inhomogeneities in the electrostatic potential. Note, however, that a crossover to the regime of dominant Coulomb interactions (see Eq. (2)) is to be expected at carrier densities around n_X where $E_{\text{kin}} \approx e^2 n_c^{1/3} / \kappa$, i.e.,

$$n_X \approx \left(\frac{e^2 / \kappa}{\hbar^2 / 2m} \right)^3. \quad (4)$$

This point is important for the quantitative understanding of the memory dip as a function of carrier density.

In the following subsection we will argue that in the high density regime of Eq. (3) the standard model of amorphous semiconductors with strongly localized electrons still applies provided a generalized localization condition is met.

In both the classical impurity band model and in amorphous semiconductors the unscreened Coulomb interactions between the localized carriers are the crucial ingredient that leads to strong electron-electron correlations. Those reflect themselves in a finite temperature glass transition and the formation of the Coulomb gap. An approximate description covering both of the standard models is given by the lattice model of localized electrons subject to the classical Hamiltonian³⁹

$$H = \sum_i n_i \epsilon_i + \frac{1}{2} \sum_{i,j} \frac{e^2}{\kappa} \frac{n_i n_j}{r_{ij}}. \quad (5)$$

Here $n_i = 0, 1$ are the occupation numbers of the lattice sites (configurations with doubly occupied states are neglected due to large “on-site” repulsion). The approximation consists in considering the disorder energies ϵ_i as *independently* and identically distributed random variables with a characteristic width W . This gives rise to a bare density of states $\nu_0 = 1/a^3 W$ where a is the lattice spacing. The classical impurity band problem corresponds to $\gamma \equiv W/(e^2/\kappa a) \approx 1$ while amorphous semiconductors are described by the limit of strong disorder, $\gamma \gg 1$. At least in the latter case, it should be irrelevant whether the underlying lattice is regular (e.g., square or cubic) or random, since the sites with low energies of the order of $e^2/\kappa a$ will be randomly distributed and emulate an effective lattice disorder (see Refs.^{40,41,42} for discussions of this point in the case $\gamma \approx 1$.)

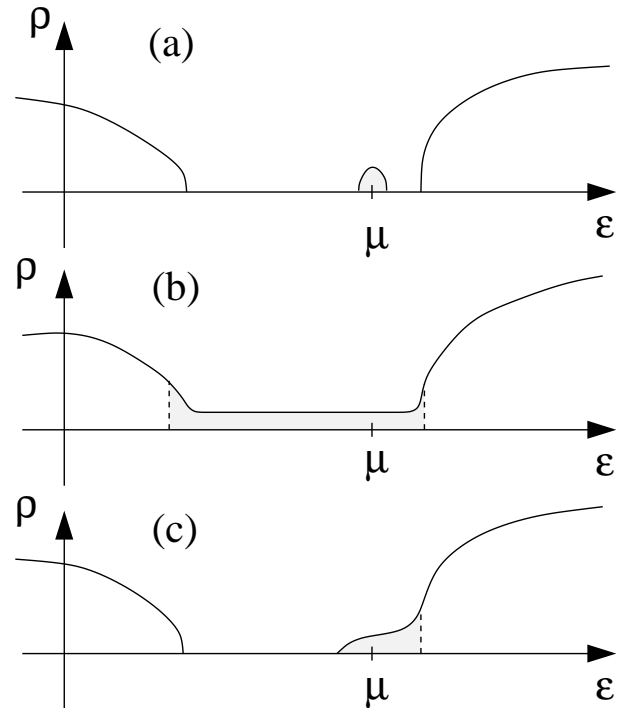


FIG. 2: Schematic view of the bare density of states (neglecting electron-electron interactions) in different classes of semiconductors: a) classical impurity band (lightly doped semiconductors) b) strongly disordered amorphous semiconductor (e.g., amorphous germanium), c) doped, disordered semiconductor with localized band tails at the bottom of the conduction band (e.g., indium-oxide).

B. Extension to systems with higher carrier density

Most of the interesting glassy effects have been observed in systems with a high density of carriers: in various granular metals and, most importantly, in indium-oxides which are highly disordered semiconductors, that can be prepared to have exceptionally high carrier densities in a huge range $n_c \approx 10^{19} - 10^{22} \text{ cm}^{-3}$ while still being insulating. It will become clear later, that a high carrier density is indeed crucial for the observability of glassy effects in the conductivity (see Section VII).

Even though the carriers are still clearly localized in these high density materials - either due to the presence of physical grains in the metal films or due to the Anderson localization in strongly disordered indium-oxides - it is not obvious that these systems can be described by the lattice model (5), since typically the number of carriers per localization volume is larger than one. We argue, however, that these high density systems can still be reduced to an effective lattice model, provided the parameter $z \equiv \nu_0 \xi^{D-1} e^2 / \kappa$ is small.

The idea is to consider only a strip of localized states of width ΔE around the chemical potential, and to write down an effective model in terms of occupied and empty levels within this strip, see Fig. 3. In this approximation,

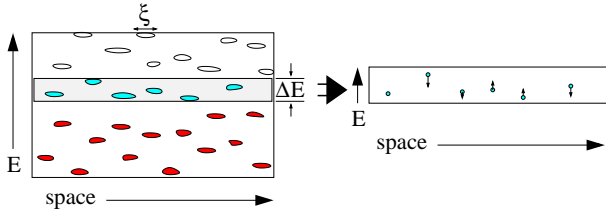


FIG. 3: The localized states in a high density system (left) spatially overlap with states at different energies. The mapping onto an effective low energy model of strongly localized electrons is carried out by freezing the electronic occupation outside an energy strip of width ΔE . The mapping is consistent provided that the fluctuating shifts of single electron energies (arrows) due to reconfigurations within the strip are smaller than ΔE .

the carriers localized in states of lower energy are considered inert in the sense that they do not hop to other sites. Notice however, that such “core” electrons may still have fairly extended wavefunctions, and therefore contribute to the polarizability of the medium, renormalizing the host dielectric constant.

The mapping of such an energy strip to a model of point-like localized states (5) makes sense only under the condition that *i*) the states within the strip do not overlap,

$$\Delta E \nu_0 \xi^D < 1, \quad (6)$$

and that *ii*) the typical variations $\delta\phi$ of the electrostatic energy due to rearrangements of particles within the strip do not exceed the width ΔE of the strip,

$$\delta\phi \sim (\nu_0 \Delta E)^{1/D} \frac{e^2}{\kappa} < \Delta E. \quad (7)$$

The conditions (6) and (7) can indeed be satisfied simultaneously, if

$$z = \frac{e^2}{\kappa} \nu_0 \xi^{D-1} < 1, \quad (8)$$

or, in other words, if the level spacing within a localization volume is larger than the Coulomb interaction strength on the scale of the localization length. Typical values for z in indium-oxides can be estimated to be of the order of $z \approx 0.2 - 0.5$. We expect that for values up to $z \approx 1$, the lattice model is a very reasonable approximation, while for $z \gg 1$ the interactions between carriers will be altered from the simple $1/r$ law since the wavefunctions within any energy strip satisfying (7) overlap significantly. In this regime, but still below the metal-insulator transition, one may expect an electron glass phase of different nature.

In granular metals, the role of the localized sites in the model (5) is obviously taken by the grains. As a consequence of impurities and the disorder in the size and the arrangement of the grains, the cost to introduce one more particle on a grain is a random quantity of

the order of the typical charging energy E_C or the level spacing δ in the grain, whichever is larger. Usually the charging energy will dominate, unless the grains are very small or the effective dielectric constant of the metallic film is very large. The random on-site energies ϵ_i entering the Hamiltonian (5) are therefore scattered with a typical width $W = \max[E_C, \delta]$, and the effective bare density of states can be estimated as

$$\nu_0 \approx \frac{n_c}{\max[E_C, \delta]}, \quad (\text{granular metals}) \quad (9)$$

which is typically a few times smaller than the (2D) density of states in a bulk metal.

When discussing Coulomb interactions, the very thin granular metal films can be considered as insulators with a very high effective dielectric constant, $\kappa \sim O(1000)$. Due to the large mismatch between κ and the dielectric constant $\kappa_s \ll \kappa$ of the surrounding media, the Coulomb interactions between charges on different grains only decay logarithmically up to distances of the order of $(\kappa/\kappa_s)d$, before crossing over to the usual $1/r$ law. As discussed by Khmelntskii and Larkin⁴³, this may lead to a strongly enhanced Coulomb gap and nearly activated conductivity as is indeed observed in many of the very thin granular metals^{14,44} for which glassy behavior was reported.

In the following, we restrict ourselves to $1/r$ -interactions. However, on a qualitative level, our arguments about the memory effect apply equally well to the granular metals.

IV. GLASS TRANSITION AND COULOMB GAP

A. The Coulomb gap

Since the pioneering works by Pollak¹⁹, Efros and Shklovskii²⁰ in the early seventies, it has been known that the unscreened Coulomb interaction in Anderson insulators lead to important correlations in the configuration of electrons, and in particular to the Coulomb gap in the single particle density of states. Based on a self-consistent stability argument, Efros³⁹ obtained an upper bound for the single particle density of states in D dimensions

$$\rho(E) = \begin{cases} \alpha_D \left(\frac{\kappa}{e^2}\right)^D E^{D-1} & E < E_C \\ \nu_0 & E > E_C \end{cases} \quad (10)$$

where

$$E_C = \left[\frac{\nu_0 (e^2/\kappa)^D}{\alpha_D} \right]^{\frac{1}{D-1}} \quad (11)$$

is the typical scale below which Coulomb correlations dominate over the disorder, and α_D is a numerical constant.

In a recent mean-field approach²¹ it has been shown that the saturation of the upper bound (10) as well as the universality of the exponent $D - 1$ are related to the occurrence of a (continuous) glass transition and the marginal stability of typical metastable states in the low temperature phase. In the limit of large disorder, $\gamma \gg 1$, the glass transition temperature for 3D systems was predicted to be^{21,22}

$$T_g^{(3D)} = \frac{1}{6(2/\pi)^{1/4}} \alpha_3^{1/2} E_C. \quad (12)$$

Generalizing the locator approximation of Ref.²¹ to 2D systems in the strong disorder limit, one obtains the prediction

$$T_g^{(2D)} = \frac{\sqrt{8\pi}}{\log\left(\frac{\sqrt{\pi/2}}{z}\right)} \alpha_2 E_C^{(2D)}, \quad (13)$$

This result should be taken with a grain of salt, however, since the locator approximation of Ref.²¹ is not as well justified as in 3D. Still, we note, that the numerical factor T_g/E_C is much larger than in the 3D case. One might therefore expect glassy behavior in strongly disordered films at temperatures where the Coulomb gap is hardly developed yet.

In the limit of weak disorder ($\gamma \approx 1$), applicable to the classical impurity band, the Coulomb correlation scale is identical to the nearest neighbor interaction strength, $e^2/\kappa r_c$. In this case, the locator approximation used in Ref.²¹ is not well justified. Applying it nevertheless, one finds a glass transition, however of a discontinuous nature (with a sudden jump in the glass order parameter). The numerical prefactor of $e^2 n_c^{1/3}/\kappa$ turns out to be of the order of 0.03 which is comparable to the small values found in simulations on irregular lattices without on-site disorder^{40,45}. We therefore expect that in lightly doped semiconductors in 3D a glass transition occurs around

$$T_g^{(3D)} \approx 0.03 \frac{e^2 n_c^{1/3}}{\kappa} \quad (14)$$

The situation for weak disorder in 2D systems is rather unclear, several authors^{46,47} claiming that there is no numerical evidence for a thermodynamic glass transition, at least for temperatures above $0.05 \alpha_2 E_C$.

As we have mentioned in section II, the experimental observation of slow relaxation in GaAs⁵ are in good agreement with the theoretical estimate (14). Similarly, we believe that the rapid drop of relaxation times in indium-oxide with the carrier density below $n_{cr} \approx 10^{19} \text{ cm}^{-3}$ is a manifestation of the glass transition. Indeed, at such low carrier densities, $n_{cr} < n_X$, indium-oxide films should be well described by the classical impurity band model, for which Eq. (2) yields a value of T_g very close to the actual measurement temperature $T_m = 4K$ (using a dielectric constant of the order of $\kappa \approx 30^{48}$). Films with $n_c < n_{cr}$ are in their ergodic high temperature phase.

B. Numerical evidence for glassy behavior

Even though the numerical evidence for a thermodynamic glass transition was only reported for a relatively special case of 3D electron glasses, out-of-equilibrium behavior in the *dynamics* of electron glasses was found in various numerical studies over the last few years. Perez-Garrido et al.⁴⁹ found a very wide distribution of relaxation times in 3D electron glasses, leading to logarithmic energy relaxation. The work of Menashe et al.^{46,50} demonstrates that even at very low temperatures there are strong fluctuations in the occupation of sites whose on-site energies lie within the Coulomb gap. This possibly indicates the presence of soft collective modes in the glass state. Tsigankov et al.³³ report a systematic positive correlation between the conductivity and the total energy of different metastable states, suggesting that the slow relaxation of conductivity is due to the descent of the system to states with lower and lower energy, involving very slow inter-state transitions. Grempel⁴⁷ found breaking of time-translational invariance (aging) and the violation of the fluctuation-dissipation relation in the Coulomb glass in 2D⁴⁷. Similar effects were reported for 3D systems by Kolton et al.⁵¹, and a strong heterogeneity of the motion of individual electrons, somewhat similar to glass-forming liquids, was observed.

Surprisingly almost no simulations have been carried out to study the glassy dynamics after charge injection into an electron glass, which, after all, is the most common experimental way to probe glassy effects. Future numerical studies in this direction would be very interesting to test the ideas presented below in section VI.

V. HOPPING TRANSPORT AND PERCOLATION THEORY

A. Percolation theory

As found by Efros and Shklovskii²⁰, at low temperatures, the appearance of a Coulomb gap profoundly alters the hopping conductivity. One can obtain a quantitative description of the hopping conductivity within a given metastable state from the standard application of percolation theory to a network of Miller-Abrahams resistors formed by pairs of sites^{52,53,54}, as reviewed in Appendix A. At high temperatures, where the hopping electrons basically probe the essentially featureless density of states above the correlation scale E_C , one finds Mott's variable range hopping law

$$R(T) = R_0 \exp \left\{ \left(\frac{T_M^{(D)}}{T} \right)^{\frac{1}{D+1}} \right\}, \quad (15)$$

where $T_M^{(3D)} = 19.4/\nu_0 \xi^3$ and $T_M^{(2D)} = 13.9/\nu_0^{(2D)} \xi^2$. At lower temperatures, the probed energy range will fall within the Coulomb gap. The depletion of the density

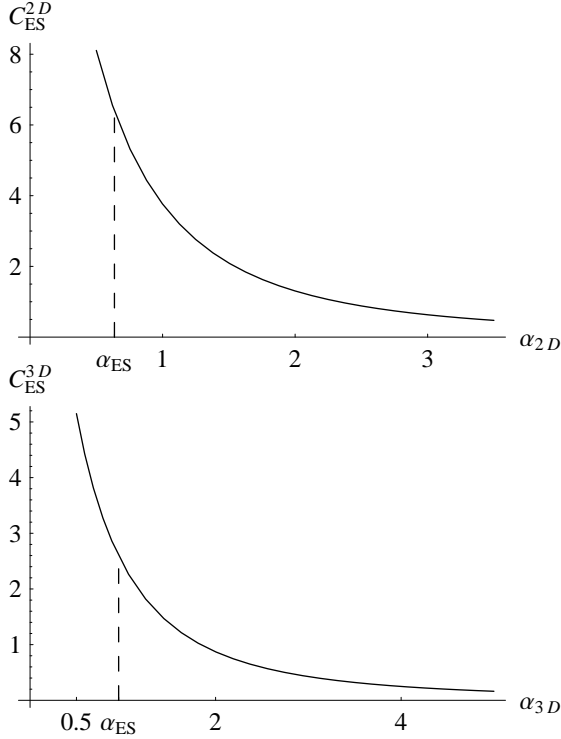


FIG. 4: The prefactors $C_{ES}^{(D)} = T_{ES}^{(D)} / (e^2 / \kappa \xi)$ as a function of α_D for dimensions $D = 2, 3$.

of states (10) results in the Efros-Shklovskii conductivity with a characteristic temperature exponent $1/2$ independent of dimensionality,

$$R(T) = R_0 \exp \left\{ \left(\frac{T_{ES}^{(D)}}{T} \right)^{1/2} \right\}, \quad (16)$$

where $T_{ES}^{(D)} = C_{ES}^{(D)} \frac{e^2}{\kappa \xi}$. The constants $C_{ES}^{(D)}$ depend on the prefactors α_D which multiply the density of states (10). The appropriate value of α_D for the quasiparticle excitations relevant for conductivity (sometimes referred to as electronic polarons³⁵) is still a matter of debate. Since for the scope of the present paper this subtlety is not very relevant, we chose to stick to Efros' prediction $\alpha_D = D/\pi$, even though the numerical study of Davies et al.³ and the mean-field theory of Müller and Ioffe²¹ both suggest values of α_D that are significantly larger. The effect of a narrower Coulomb gap on the prefactors $C_{ES}^{(D)}$ is shown in Fig. 4.

It is instructive to see how the characteristic energies E_C , T_g , T_{ES} and T_M scale with the localization parameter z , cf. Eq. (8). One easily finds $T_g/E_C = O(1)$ [$\sim 1/\log(z)$ in 2D], $T_{ES}/E_C \sim 1/z^{1/(D-1)}$ and $T_M/E_C \sim 1/z^{D/(D-1)}$. Again, the condition $z \ll 1$ is necessary to insure a clear separation of energy scales.

Considering a quasiparticle density of states of the form (10) and applying the percolation arguments of appendix A, one easily obtains a crossover function

$$\log R(T) = z^{-1/(D-1)} \mathcal{R}(T/T_X), \quad (17)$$

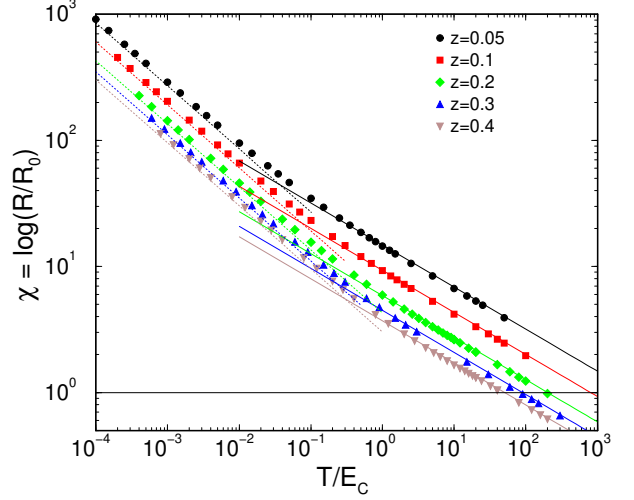


FIG. 5: Crossover from Mott to Efros-Shklovskii conductivity for different values of the parameter z . The points were calculated with the percolation approach of App.A and the temperature dependent density of states of Eq.(28) for the 2D case. The straight lines correspond to the asymptotics given in Eqs.(A9) (A10).

where

$$T_X = (T_{ES}^{D+1} / T_M^2)^{1/(D-1)} \sim z^{1/(D-1)} E_C \quad (18)$$

is the temperature at which Mott's law (15) crosses over to the Efros-Shklovskii regime (16). The resulting curves are shown in Fig. 5 for a 2D system with varying localization parameter z . (We used the density of states (28) described below). In the literature a variety of such "universal" crossover curves have been discussed^{55,56}. They differ in the precise form of the quasiparticle density of states and the percolation criterion employed which results in slightly different numerical prefactors for the values of T_M and T_{ES} , as well as in subtle differences in the detailed shape of the function \mathcal{R} close to the crossover.

Even though the crossover from Mott- to Efros-Shklovskii hopping is readily observed in semiconductor systems sufficiently close to the metal-insulator transition^{24,57}, it is very difficult to extract non-trivial information on the nature of Coulomb correlations or the shape of the Coulomb gap from fitting them to crossover functions like (17). This is so because the asymptotics (15), (16) allow at most to determine two of the parameters ν_0 , ξ and κ which are usually not known independently with sufficient accuracy to test the numerical factors $C_{M,ES}$ from percolation theory. In order to infer more information about the details of the quasiparticle density of states, one needs a high experimental resolution of the crossover around T_X , and an unbiased way to discriminate between different percolation criteria.

It turns out, however, that *differential* measurements such as memory and aging experiments in the glassy regime contain direct information on correlations since they are only sensitive to *changes* in the electron configuration as some external parameter is varied. As long as

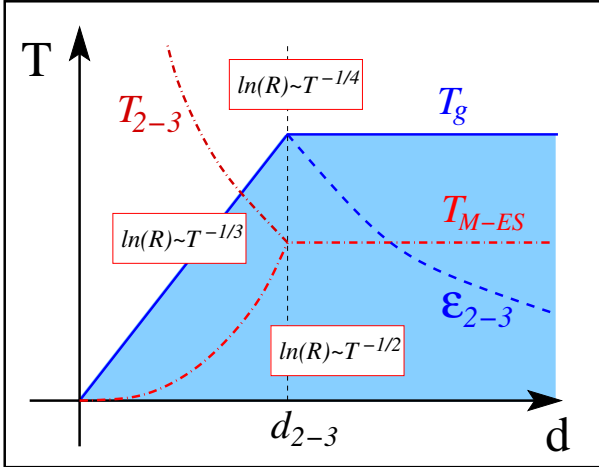


FIG. 6: Phase diagram of (strongly disordered) electron glasses as a function of temperature and film thickness. The red lines indicate the crossover between different hopping regimes. The blue lines separate the ergodic high temperature phase from the glass phase where memory effects and aging are observable. The dashed line indicates the temperature and energy scale below which the density of states assumes a linear shape characteristic for two dimensions.

one stays in the glassy phase, $T < T_g$, these experiments allow to probe Coulomb correlations even in the Mott regime where Coulomb effects can hardly be seen in the *global* behavior of the resistivity $R(T)$.

B. Considerations of dimensionality

In this section we briefly discuss the crossover film thickness d_{cr} below which a sample should be considered two-dimensional. As we discuss below, the crossover from a bulk (3D) sample to a film is governed by

$$d_{cr} \sim (\nu_0 e^2 / \kappa)^{-1/2}, \quad (19)$$

both with respect to hopping transport and the glass transition. Using typical values for indium-oxide films ($\nu_0 \approx 10^{32} \text{ erg}^{-1} \text{ cm}^{-3}$ and $\kappa \approx 30$) one finds $d_{cr} \sim 100 \text{ \AA}$ which is of the order of the typical film thickness ($d = 50 - 200 \text{ \AA}$) in most glassy experiments.

In a thin film, Mott's variable range hopping law (15) crosses over from the 3-D form ($\log(R) \sim T^{-1/4}$) to the 2-D form ($\log(R) \sim T^{-1/3}$) when the hopping length becomes of the order of the film thickness, which yields the crossover temperature

$$T_{2D-3D} \sim T_M^{(3D)} (\xi/d)^4 \sim T_X^{(3D)} / (\nu_0 d^2 e^2 / \kappa)^4. \quad (20)$$

A subsequent crossover to the Efros-Shklovskii law takes place at $T_X^{(2D)} = T_X^{(3D)} (\nu_0 d^2 e^2 / \kappa)$, where $T_X^{(3D)}$ denotes the Mott to Efros-Shklovskii crossover temperature for a bulk sample. The intermediate regime with a 2D-Mott's law is observable only if $d < d_{cr}$.

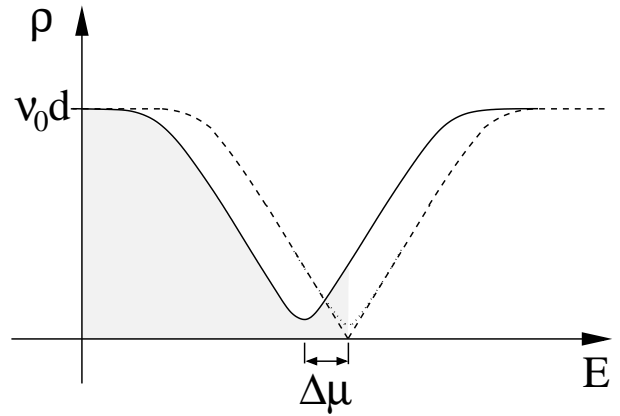


FIG. 7: A sketch of the density of states in a 2D electron glass. The dashed curve corresponds to zero temperature. The dotted curve shows the result of thermal smearing, cf. Eq.(28). The solid curve represents the density of states immediately after applying a gate voltage, cf. Eq.(31). $\Delta\mu$ is the shift of the chemical potential due to the charging of the sample.

The crossover from a 3D to a 2D glass transition occurs when the typical distance between thermally active sites at $T = T_g^{(3D)}$ becomes equal to the film thickness, i.e., when

$$R_{T_g} \sim e^2 / \kappa / T_g^{(3D)} \sim e^2 / \kappa / T_g^{(2D)} \quad (21)$$

does. One easily checks that these expressions all become of the same order when $\nu_0 d^2 e^2 / \kappa = (d_f / d_{cr})^2 \approx 1$. Notice that for films with $d < d_{cr}$, the glass transition temperature (13) decreases roughly linearly with thickness since $T_g^{(2D)} \sim \nu_0^{(2D)} \sim d \nu_0$ (in the following we denote the bulk density of states by ν_0). The phase diagram of electron glasses as a function of temperature and film thickness is summarized in Fig. 6.

VI. THEORY OF THE MEMORY DIP

A. The density of states as a function of T and V_g

As discussed in details in Section IV, the two-dimensional density of states exhibits a linear Coulomb gap at low temperatures. At energies larger than the Coulomb correlation scale $E_C = \alpha_2^{-1} (e^2 / \kappa)^2 \nu_0 d$, the density of states approaches the constant bare density of states $\nu_0^{(2D)} = \nu_0 d$. We describe this crossover (for $T = 0$) by the interpolating function

$$\rho_0(E) = \nu_0 d \tanh |E/E_C|, \quad (22)$$

whose precise form is not essential for the following analysis.

At finite temperature some electrons are excited out of their local equilibrium position, which induces fluctuations in the site energies, $E_i = \epsilon_i + \sum_{j \neq i} e^2 n_j / \kappa r_{ij}$:

$$E_i = E_i^{(0)} + \delta \phi_i \quad (23)$$

where

$$E_i^{(0)} = \epsilon_i + \sum_{j \neq i} e^2 n_j^{(0)} / \kappa r_{ij} \quad (24)$$

is the excitation energy of site i in the local ($T = 0$) minimum configuration ($\{n_i^{(0)}\}$), and

$$\delta\phi_i = \sum_{j \neq i} e^2 \delta n_j / \kappa r_{ij} \quad (25)$$

are Coulomb fluctuations due to thermally activated changes in the occupation δn_j . In a first approximation we assume the $\delta\phi_i$'s to be independent Gaussian distributed variables with variance $\langle \delta\phi^2 \rangle = \alpha_T n_T (e^2 / \kappa)^2$,

$$P_T(\delta\phi) = \frac{\kappa}{e^2 \sqrt{\pi \alpha_T n_T}} \exp \left\{ -\frac{\kappa^2 \delta\phi^2}{e^4 \alpha_T n_T} \right\}, \quad (26)$$

where $\alpha_T = O(1)$ is a numerical factor and n_T is the density of thermally excited electrons

$$n_T = \int_{-\infty}^0 dE \rho_0(E) (1 - f(E)) + \int_0^\infty dE \rho_0(E) f(E), \quad (27)$$

f being the Fermi distribution. Note that at high temperatures n_T is linear in T , while at low temperatures it approaches zero like $n_T \sim T^2$, due to the Coulomb gap.

As a consequence of these fluctuations, the density of states is smeared. In the above approximation of independent shifts $\delta\phi_i$, it is described by the convolution.

$$\rho(E, T) = \int d(\delta\phi) P_T(\delta\phi) \rho_0(E - \delta\phi), \quad (28)$$

The resulting density of states reproduces the qualitative features found in the extensive numerical study of Ref.⁵⁹.

When a gate voltage V_g is applied, the carrier density of the sample is changed. If the system is given a long time to equilibrate, it will settle in the new ground state corresponding to V_g , with the Coulomb gap shifted to a new chemical potential. However, in most experiments the sample is probed on much shorter time scales, so that one can approximate the change of density of states due to gate voltage as nearly instantaneous. Neglecting any partial relaxation processes, the effects of the gate voltage are twofold: *i*) the new carriers successively fill the empty levels close to the Fermi energy, shifting the chemical potential to $\mu + \Delta\mu$, while the minimum in the density of states remains at the old value of μ ; *ii*) the extra particles further smear the density of states, similarly to the thermal effect described above. They induce new energy shifts $\delta\phi_i$, which we again take to be randomly distributed according to

$$P_{V_g}(\delta\phi) = \frac{\kappa}{e^{3/2} \sqrt{\pi \alpha_V C V_g}} \exp \left\{ -\frac{\kappa^2 (\delta\phi - \Delta\mu)^2}{e^3 \alpha_V C V_g} \right\}, \quad (29)$$

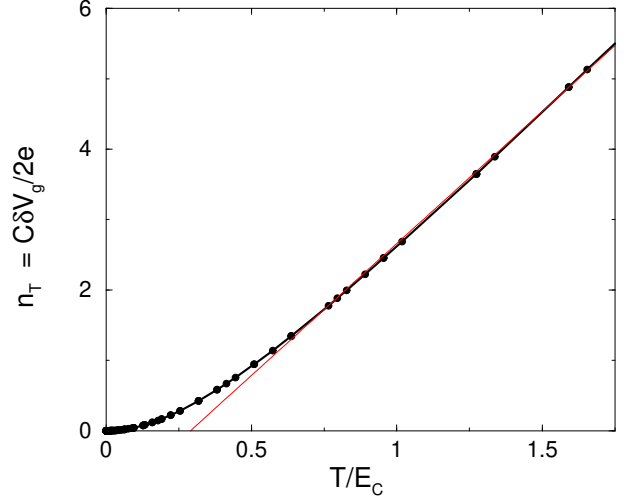


FIG. 8: The density of thermally excited carriers, n_T , as a function of temperature, or equivalently, the gate voltage difference $C\delta V_g/e$ at which the anomalous field effect saturates. At high temperature, δV_g is linear in T , and scales as T^2 at low temperatures. n_T and $C\delta V_g/e$ are plotted in units of $zE_C\nu_0d$.

where $\alpha_V = O(1)$, C is the capacitance per unit area. Here we have also accounted for the global shift in chemical potential $\Delta\mu$, which is related to the gate voltage by

$$CV_g = e \int_0^{\Delta\mu} dE \rho(E). \quad (30)$$

Notice that due to the presence of the Coulomb gap, the dependence of $\Delta\mu$ on V_g is non-linear. The density of states after a sudden gate voltage change is finally obtained as

$$\rho(E, T, V_g) = \int d(\delta\phi) P_{V_g}(\delta\phi) \rho(E - \delta\phi, T, V_g = 0). \quad (31)$$

The density of states at different stages of smearing is shown in Fig 7.

One might worry that assumption *i*) is not justified since the equilibrium screening length, is much smaller than the typical film thickness, resulting in all new carriers migrating to the film surface. However, as we will discuss in more details in Section VII A, the relaxation to this equilibrium state is a very slow process, while on shorter time scales, relevant for memory experiments, the extra charges are almost homogeneously distributed across the sample.

B. Instability criterion and breakdown of memory

The above description of an adiabatic response to the change of gate voltage V_g , without any relaxation of the electron configuration, is applicable only for small enough values of V_g . As the gate voltage is increased, more

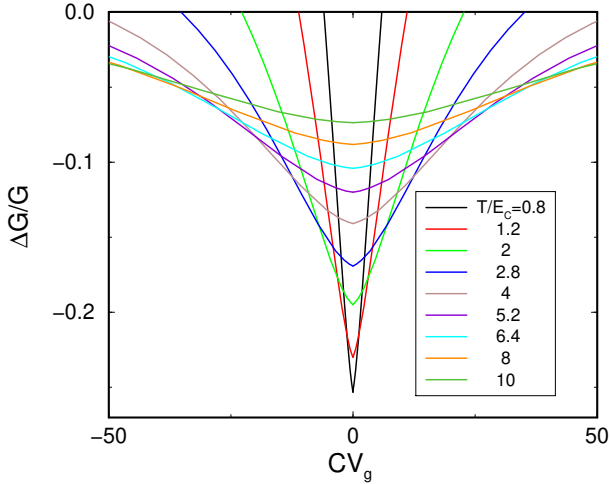


FIG. 9: Memory dip as a function of gate voltage for $z = 0.4$ and various temperatures of the order of E_C and higher. We plot the relative change in conductivity with respect to its asymptotic value at large gate voltages, $\Delta G/G = [G(V_g) - G(V_{\text{ins}})]/G(V_{\text{ins}})$. The cusp width is proportional to temperature, and its amplitude decreases as temperature is increased. CV_g is plotted in units of $ezE_C\nu_0d$

and more new particles are introduced into the sample and reshuffle the site energies, until at a certain point ($V_g = V_{\text{ins}}$) the local minimum in which the system resides becomes unstable. For higher gate voltages the system will relax to a new local minimum whose density of states is not adequately described by the adiabatic smearing and shifting of Eq. (31) alone. As long as the Coulomb gap is not very strongly developed, it is reasonable to assume that the new local minimum represents a rather generic metastable state which is relatively high up in the energy spectrum of all possible states at that gate voltage. One therefore expects that the conductivity will not significantly change upon further increase of the gate voltage, since the system always remains in the high energy spectrum of metastable states. However, it is important to note, that the new metastable state will still have a large configurational similarity (or ‘overlap’ in spin glass language) with the original ground state (*i.e.*, most of the sites that were occupied in the original local state remain occupied in the new local minimum). The memory of the original configuration is thus preserved, in particular, when the gate voltage is swept back to its original value, the low equilibrium conductivity will be recovered. As the gate voltage is increased beyond the instability scale V_{ins} , the overlap of the new local minimum with the original state continuously decreases and the memory of the original state is gradually lost. This will manifest itself by the complete disappearance of the memory dip once the gate voltage is swept beyond a scale V_{mem} . One expects that at a similar scale the simple (t/t_w) -scaling observed in aging experiments¹² will break down.

Let us now analyze in more detail what determines

the instability scale V_{ins} . It is reasonable to expect that as long as the density of carriers introduced by the gate is smaller than the density of thermally excited electrons n_T , the gate voltage effect is perturbative, which justifies our adiabatic treatment of the density of states. This reasoning implies $CV_{\text{ins}} \gtrsim en_T$.

On the other hand, at gate voltages $CV_g > en_T$ the shift in chemical potential is of the order of the temperature $\Delta\mu \sim T$, and accordingly, the new carriers are introduced on sites that were essentially always empty in the original state. The local environment of those sites will generally not be in a configuration which is favorable to the addition of a new particle. Rather, the newly introduced electron will trigger relaxation processes and thus destabilize the original state. In other words, the configuration generated by occupying the sites close to Fermi level will soon become a generic high energy state beyond $CV_g > en_T$. We thus conclude that,

$$V_{\text{ins}} \approx \frac{en_T}{C} \approx \frac{e\nu_0d}{C} \times \begin{cases} \pi^2 T^2 / 6E_C & T \ll E_C \\ 2\ln 2 T - \Omega / 2\nu_0d & T > E_C \end{cases} \quad (32)$$

where $\Omega = \int dE(\nu_0d - \rho(E)) \sim \nu_0dE_C$ is the volume of the Coulomb gap. As explained above the memory dip around $V_g = 0$ is expected to saturate around the instability scale, and its width is thus roughly $\delta V_g = 2V_{\text{ins}}$, see Fig. 8. The linear high temperature behavior $\delta V_g \sim T - T_0$ was indeed observed experimentally⁴⁸. Equation (32) predicts the interesting relation $T_0 = \int dE(1 - \rho(E)/\nu_0d)/4\ln 2$, which allows to determine experimentally the volume of the Coulomb gap.

As mentioned above the memory of the equilibrium state is essentially erased once the gate voltage exceeds a certain scale $V_{\text{mem}} > V_{\text{ins}}$. This crossover scale will be reached when the original Coulomb gap is smeared out completely by the random energy shifts $\delta\phi_i$ due to new carriers, *i.e.*, when $\langle\delta\phi_i^2\rangle \approx E_C$. More explicitly we obtain the estimate

$$V_{\text{mem}} \approx \zeta_V \frac{e\nu_0d}{C} E_C, \quad (33)$$

which is temperature independent contrary to V_{ins} . The numerical factor ζ_V is probably relatively large (at least of the order of T_g/E_C which may be large in real 2D systems with strong disorder, cf. (13)). For gate voltages $V_g > V_{\text{mem}}$, the typical single particle energy shifts are of the same order as the scale of Coulomb correlations, E_C . Thus, most correlations that have established during the equilibration will be broken up in the process of fast relaxation processes triggered by the new particles and memory is lost irreversibly. In Ref.¹¹ the authors reported that the ratio $V_{\text{mem}}/V_{\text{ins}}$ is not a universal number (at fixed temperature), but increases with carrier density. The above arguments indeed suggest that at high temperatures, $T \gtrsim E_C$,

$$\frac{V_{\text{mem}}}{V_{\text{ins}}} \propto \frac{E_C}{T - T_0}, \quad (34)$$

which increases with carrier concentration as E_C does.

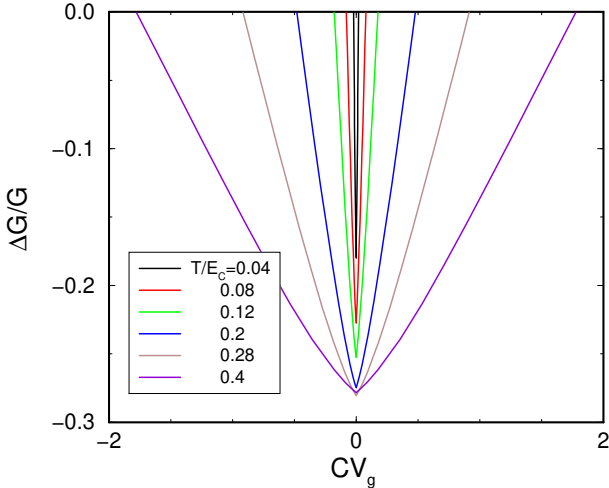


FIG. 10: $\Delta G/G = [G(V_g) - G(V_{\text{ins}})]/G(V_{\text{ins}})$ plotted against gate voltage, for low temperatures, $T < E_C$, and $z = 0.4$. In this regime, the cusp width increases quadratically with temperature. The adiabatic percolation treatment predicts the amplitude of the cusp to increase with temperature. This is probably an artifact, see the discussion in Section VII. CV_g is plotted in units of $ezE_C\nu_0d$.

C. Non-equilibrium conductivity

In experiments, the memory dip is observed by monitoring the film conductivity as the gate voltage is swept through the equilibration point. The sweep rate is usually much faster than the relaxation time of the glassy sample. For gate voltages below V_{ins} we can calculate the non-equilibrium conductivity from the modified density of states, Eq. (31), and the percolation criterion of Appendix A. Assuming that the conductivity saturates to G_∞ beyond the scale V_{ins} , we may estimate $G_\infty \approx G(V_g = V_{\text{ins}})$ from which we obtain the amplitude of the memory dip as $\Delta G \equiv G_\infty - G(0) \approx G(V_{\text{ins}}) - G(0)$.

We note that the smearing of the density of states due to new carriers has a minor effect on the non-equilibrium conductivity since it mostly affects energy scales on the order of the temperature whereas the energy range probed by variable range hopping is much larger. However, the shift of the chemical potential, $\Delta\mu$ is the crucial feature which leads to the increase of the conductivity.

The results of the percolation approach are consistent with the general assertion⁸ that the conductivity always increases with $|V_g|$. The latter is reflected in a rather sharp dip around $V_g = 0$ where the system was equilibrated. In Fig. 9 we plot the relative change of the conductivity $\Delta G(V_g)/G_\infty$ for high temperatures $T_g > T \gtrsim E_C$.⁵⁸ This is the temperature regime in which most experiments on indium-oxide films are performed. The cusp width increases linearly with temperature while its amplitude decreases.

In Fig. 10 we plot the same observable $\Delta G(V_g)/G_\infty$ for $T < E_C$. In this regime the cusp width increases

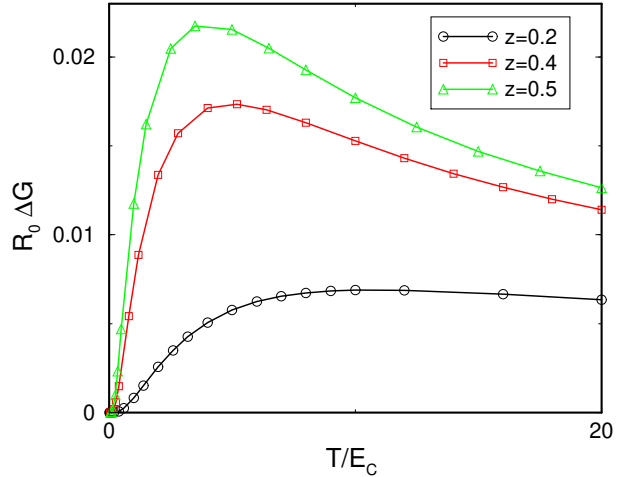


FIG. 11: Amplitude of the conductivity dip $G(V_{\text{ins}}) - G(0)$, as a function of temperature for $z = 0.2, 0.4$ and 0.5 . Less resistive films (larger z) exhibit a clear maximum at relatively high temperatures.

quadratically with temperature. In contrast to the high temperature regime, the adiabatic percolation treatment predicts $\Delta G(V_g)/G_\infty$ to increase with temperature. Such a non-monotonic behavior of the *relative amplitude* was not observed in experiments so far. This might be due to the fact that most experiments are performed at high temperatures. However, we believe that our approximations are not fully justified at low temperatures and the predicted decrease of $\Delta G(V_g)/G_\infty$ might be an artifact. In particular, the estimate $G_\infty \approx G(V_{\text{ins}})$ is probably too small as we shall discuss in Section VII.

In general, the *absolute amplitude* of the dip, ΔG , is found to be a non-monotonic function of temperature as is clearly seen in Fig. 11. The non-monotonicity is more pronounced in less resistive films ($z = 0.4, 0.5$ where a clear peak appears in ΔG at T_{max} , while for more resistive cases ($z = 0.2$) this feature is hard to discern. Very similar non-monotonic behavior of ΔG was observed experimentally in Ref.¹⁸. Moreover, if we fit the percolation result for T_{max} to a power law as a function of the localization length ξ ($\sim z$), as was done by those authors, we find similar exponent $T_{\text{max}} \sim z^{-\nu}$ with $\nu \approx 1$, see Fig. 12. We have, however, no analytical justification for such a power law behavior.

Finally, let us discuss the relative amplitude of the conductivity dip $\Delta G/G$ as a function of temperature, cf. Fig. 13. At high temperatures it decays with temperature, approaching the asymptotics

$$\frac{\Delta G}{G} \sim \frac{E_C}{T}. \quad (35)$$

At very low temperatures, the percolation approach predicts that $\Delta G/G$ increases with temperature, and an asymptotic analysis shows that

$$\frac{\Delta G}{G} \sim \sqrt{\frac{T}{T_{ES}}}. \quad (36)$$

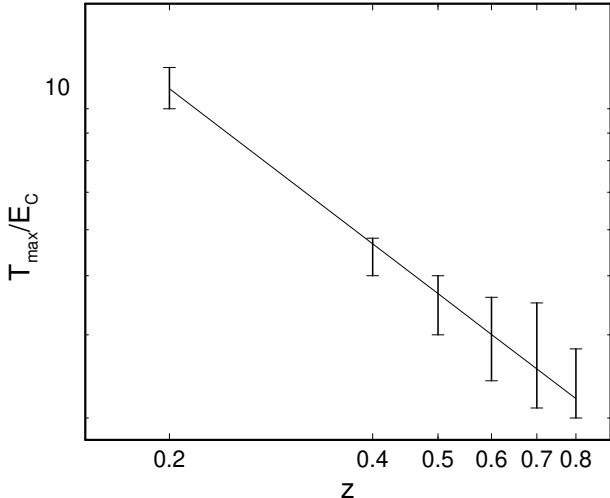


FIG. 12: The temperature T_{\max} at which ΔG is maximal, as a function of the localization parameter z . The solid line is the best fit to a power law $T_{\max} \sim z^{-\nu}$ with exponent $\nu = -1.09$.

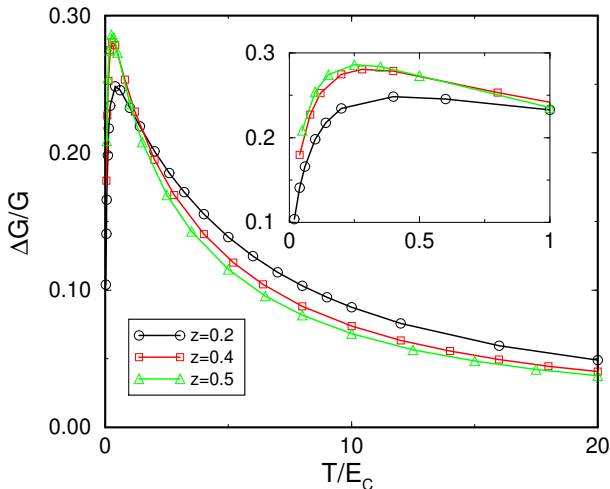


FIG. 13: The relative amplitude of the conductivity dip $[G(V_{\text{ins}}) - G(0)]/G(V_{\text{ins}})$ as a function of temperature for various values of z . Inset: Low temperature behavior of the relative amplitude for the same values of z .

The crossover between (35) and (36) occurs at relatively low temperatures (of the order of the Mott - Efros-Shklovskii crossover T_X). However, as already mentioned, Eq. (36) might significantly underestimate the true amplitude of the memory dip.

VII. DISCUSSION

A. Spatial distribution of induced carriers

In the derivation of the adiabatically modified density of states, we assumed that the gate induced carriers are distributed over the whole sample and *not* confined in

a thin surface layer of the order of the Thomas-Fermi screening length. As we discussed in Sec. II, the carriers will on average be located within a distance of the order of $\Delta n^{-1/2}$ from the sample surface, where Δn is the density of excess carriers. Only after very slow relaxation processes the system will find its new ground state where indeed the excess charge will be concentrated much closer to the surface.

A typical value for the density of induced carriers in indium-oxide experiments¹² is $\Delta n \approx 3 \cdot 10^{10}/\text{cm}^2$ (corresponding to V_{ins}), which yields a typical distance between induced carriers $l_{cc} \sim \Delta n^{-1/2} \approx 600\text{\AA}$, which is larger than the sample thickness d in most of the experiments. For samples thicker than l_{cc} , the gate voltage gradually becomes a surface perturbation. In order to describe this effective 3D-regime, the approach presented above would have to be revised in order to account for an inhomogeneous density of states across the sample.

B. Shortcomings of the percolation approach

There are two main shortcomings in our percolation approach. First, as mentioned in the previous section, our treatment breaks down in the low temperature limit, and the prediction $\Delta G/G \rightarrow 0$ for $T \rightarrow 0$ is unphysical for the following reasons: *i*) One can trace back the origin of the prediction $\Delta G/G \sim T^{1/2}$ to the conservation of the volume of the Coulomb gap under application of a gate voltage, which in our approximation is a trivial consequence of only shifting and convoluting the density of states. However, one can easily imagine that fast relaxation processes that we have neglected would increase the density of states in the Coulomb gap when a sufficiently large gate voltage $V \sim V_{\text{ins}}$ is applied. Such a contribution would lead to the saturation of $\Delta G/G$ to a constant at low temperatures. *ii*) The assumption that the asymptotic conductivity G_∞ is well estimated by the non-equilibrium conductivity at V_{ins} is probably incorrect at very low temperatures: Imagine to apply a large gate voltage V_L much larger than V_{ins} such that $\Delta\mu$ is of the order of E_C , but still small enough to preserve some memory of the original state, $V_L < V_{\text{mem}}$. This will take the system into a new high energy state where fast relaxation processes lead to the formation of a new Coulomb gap that has almost no overlap (in energy space) with the old one. It is likely that the volume of this new gap is smaller than the one in the equilibrium state. More precisely, one may expect that the linear slope α_{ES}^{2D} of the density of states in the new configuration is larger than that in the ground state, and the resulting Efros-Shklovskii temperature T_{ES} is smaller accordingly. One immediately concludes that in this case $\Delta G/G$ should scale like $T^{-1/2}$ and thus *increase* with decreasing temperature. This would indicate that the metastable states which the system visits just beyond the instability point $V_g \gtrsim V_{\text{ins}}$, have a better developed (deeper) Coulomb gap than the real asymptotic states corresponding to larger

gate voltage. This is indeed natural to expect since for $V_g = V_{\text{ins}}$ the shift $\Delta\mu \approx T$ of the Coulomb gap is much smaller than the gap width E_C .

In conclusion, at very low temperatures, we expect an additional increase of conductivity with increasing gate voltage, even beyond the instability point V_{ins} . The description of the conductivity in that regime would however require to take into account partial relaxation processes which goes beyond the present approach. The question whether the predicted \sqrt{T} behavior at low temperatures may still have some range of validity at intermediate temperatures remains open.

The second shortcoming of the percolation approach is the neglect of spatial correlations between the energy shifts $\delta\phi_i$ due to new carriers. As discussed above in Sec. VII A the distance between nearest induced carriers, l_{cc} is typically of the order of several hundred Ångstroms. Over this length the shifts $\delta\phi_i$ are positively correlated. If the hopping length is shorter than l_{cc} , as is most often the case, the correlations reduce the amplitude of the anomalous field effect with respect to our estimate which assumed statistically independent shifts.

C. Comparison to experiments

1. The memory dip

As described in Section VI C, the adiabatic percolation approach reproduces well the temperature dependence of several key features of the memory dip, in particular we showed that from a careful study of the temperature dependence of the width one may infer the volume of the Coulomb gap.

Moreover, from Eq. (32) we see that the width of the memory dip should be proportional to the bare density of states $\nu_0 d$, whose dependence on carrier concentration was discussed in Section III A: in the impurity band regime, $n_c < n_X$, the density of states increases with n_c as $\nu_0 \sim n_c^{2/3}$, while for large carrier concentration it crosses over to $\nu_0 \sim n_c^{1/3}$. This scenario agrees rather well with the observed bending of the dip width as a function of carrier density in indium oxide films⁷.

At high temperatures, the percolation approach predicts a decrease of the cusp amplitude like $1/T$, which is weaker than what is usually observed in experiments^{14,18}. This difference may again originate from our neglect of spatial correlations in $\delta\phi_i$ discussed above. Even more likely is the scenario that our assumption of homogeneously glassy samples breaks down at higher temperatures. Indeed, if only a few rare regions with stronger disorder remain glassy their effect on the out of equilibrium conductivity might be strongly reduced due to shortcuts by non-glassy regions.

Let us briefly discuss the effect of varying the disorder strength or applying a magnetic field. Both changes seem not to affect the width of the memory dip. Furthermore the even strong magnetic fields change the amplitude

$\Delta G/G$ only slightly. These experimental observations are quite surprising since the variation of disorder and magnetic field both modify appreciably the conductivity G itself. The first observation receives a natural explanation within the picture proposed above if we make the assumption that changing the disorder (by annealing) or applying a magnetic field mostly affect the localization length, without altering the bare density of states. Since the instability criterion originates from a static consideration of a classical electron problem, it is independent of the localization length, and the width of the memory dip is thus essentially constant under variations of disorder and magnetic field.

The near constancy of $\Delta G/G$ with magnetic field is more subtle. In the language of the percolation approach the variation of the localization length simply changes the parameter z , while leaving E_C fixed. From Fig. 13, it can be seen that the effect of z on $\Delta G/G$ is indeed relatively minor, while the corresponding change of ΔG is important.

2. Memory of temperature

An interesting effect of temperature memory was reported both for the indium oxide films¹², and for films of granular aluminum¹⁷. After equilibration at $V_g = 0$ temperature T_0 , the temperature is reduced to $T_1 < T_0$, and the conductivity as a function of gate voltage is probed without letting the sample equilibrate. The anomalous field effect is then observed to have still the same characteristic width as the one at the initial temperature T_0 . This effect can be understood rather naturally in terms of the instability criterion that we proposed in the previous section: The energy minima or valleys in which the electron glass typically settles at temperature T_0 will be stable upon injection of additional carriers up to the critical density n_{T_0} . A temperature quench will not take the system out of this valley immediately, and the stability threshold of the higher temperature will be preserved for some time. Slow relaxation will finally allow the system to dig itself deeper down into the energy landscape, since the thermal fluctuations are smaller. The lower lying states will have a reduced stability threshold, and the temperature memory will eventually be lost.

3. Granular metals

Even though we carried out most of the quantitative analysis for the explicit case of two-dimensional contiguous semiconductor films, the general picture proposed for the memory dip applies equally well to granular metals. As mentioned earlier, the temperature dependence of the conductivity is strongly suggestive of a harder Coulomb gap than the linear Efros-Shklovskii gap, possibly due to logarithmic Coulomb interactions in the granular film. Experiments are then naturally carried out in the low

temperature regime, where a modified version of Efros-Shklovskii conductivity occurs. Accordingly, one would expect the width of the memory dip to have a stronger dependence on temperature (analogous to the low temperature part of Eq. (32), but with a bigger temperature exponent).

D. Observability of glassy effects in doped semiconductors

Slow relaxation was observed only in very few (moderately) doped semiconductors so far, the only well-documented case known to us being the experiment on GaAs⁵ discussed in Section II. The question then naturally arises why glassy effects, such as in indium-oxide, are not more frequently encountered. The reason is most likely that many standard semiconductors have relatively low carrier concentrations with well localized electrons. Such systems are described by the classical impurity band model whose glass transition in 3D is suppressed by a very small numerical factor, as discussed in Section IV. Estimating the Efros-Shklovskii-type conductivity at that temperature scale, one finds

$$\ln(R/R_0) \approx \left(C_{ES}^{(3D)} \frac{e^2}{\kappa \xi T_g} \right)^{1/2} \approx \left(\frac{C_{ES}^{(3D)} n_c^{-1/3}}{0.03} \frac{\xi}{\xi} \right)^{1/2}, \quad (37)$$

which is very large even when the localization length approaches the inter-impurity distance and we take a value of C_{ES} somewhat smaller than the standard Efros-Shklovskii prediction 2.8. This makes the detection of glassy signals above the noise background almost impossible. However, in such systems glassiness should still be observable in static quantities, as was demonstrated by the capacitance measurements of Ref.⁵. In amorphous semiconductors with relatively high carrier concentration glassy effects as described in this paper should generally be observable. The same is true for doped crystalline semiconductors sufficiently close to the metal insulator transition. However, when the localized wavefunctions start to overlap significantly ($z > 1$) one may expect the nature of the glass phase to change.

VIII. CONCLUSION

We have analyzed the memory effect in two-dimensional electron glasses. The non-equilibrium conductivity was calculated within a percolation approach, taking into account the non-ergodicity of the glass state and the ensuing persistence of Coulomb correlations. This allows for a quantitative description of the anomalous field-effect. Our approach reproduces many of the experimental characteristics observed in indium-oxides and granular aluminum. We have provided a simple physical picture for the voltage scales at which the mem-

ory dip saturates and erasure of memory occurs, respectively. Their ratio is predicted as a function of temperature and carrier density, which can be tested in experiments. Furthermore, we have shown that the temperature dependence of the saturation voltage can be used to extract the volume of the Coulomb gap.

IX. ACKNOWLEDGMENTS

We acknowledge discussions with M. Feigel'man, M. Gershenson, T. Grenet, L. Ioffe, Z. Ovadyahu and B.I. Shklovskii. We thank L. Ioffe and Z. Ovadyahu for the continuous encouragement and interest in our work, as well as for the frequent exchange of ideas. E.L. was supported by DOE grant DE-FE02-00ER45790. M.M. was supported by NSF grant DMR 0210575.

APPENDIX A: PERCOLATION THEORY OF HOPPING CONDUCTIVITY

We consider the network of Miller-Abrahams resistors formed by pairs of sites i and j . In the vicinity of a given low temperature metastable state of the electron glass, the effective resistance of this link is approximately given by

$$R_{ij} \approx \exp(-2r_{ij}/\xi + \epsilon_{ij}/T) \quad (A1)$$

where

$$\epsilon_{ij} = \begin{cases} |E_i - E_j| - e^2/\kappa r_{ij}, & \text{if } E_i \cdot E_j < 0 \\ \max\{|E_i|, |E_j|\}, & \text{if } E_i \cdot E_j > 0 \end{cases} \quad (A2)$$

and E_i is the energy (with respect to the chemical potential) to remove or add a particle at the site i in the particular metastable state at hand. More precisely, the energies E_i refer to the excitation of quasiparticles (or polarons) that carry the hopping current. Those are believed to be single site excitations at a site i , that are accompanied by the simultaneous short-ranged hops of few electrons close to that site, see, e.g., Ref.³⁵.

To find the least resistive percolating path in the resistor network we follow the procedure proposed by Efros et al.⁵⁴: We consider only resistors with $R_{ij} < \exp(\chi_c)$ to be active and associate to each of them a disk or ball with diameter R_{ij} . We finally determine the threshold value of χ_c for which the set of disks percolates. This yields a good estimate of the resistivity to exponential accuracy.

To solve this problem analytically, one needs to know the probability $F(\omega, r)$ per unit energy and volume to find a pair of sites (i, j) with $r_{ij} = r$ and $\epsilon_{ij} = \omega$. Under the assumption that the site energies E_i are independently distributed according to a single-quasiparticle density of states $\rho(E)$, we obtain

$$F(\omega, r) = \frac{1}{2} \int \rho(E_1) \rho(E_2) \delta(\epsilon_{12} - \omega) dE_1 dE_2. \quad (A3)$$

The assumption of uncorrelated energies has been highly debated in the literature, see, e.g. Ref.⁶⁰. We believe, however, that it is justified as long as the distance r much larger than the nearest neighbor distance (as is the case for typical hopping distances). This is so because the long range interactions assure that the two sites each interact independently with many other sites, and should therefore not be strongly correlated among each other. With the help of the pair distribution function the above percolation problem reduces to that of a set of balls with different radii. Assuming that the critical volume fraction of the balls, Θ_D , is an approximate invariant of temperature, only dependent on dimensionality, we finally have to solve the equation

$$\Theta_D = \int d\omega d^D r V_D \left(\frac{r}{2}\right)^D F(\omega, r) \theta(\chi_c - \frac{\omega}{T} - \frac{2r}{\xi}), \quad (\text{A4})$$

where V_D is the volume of a D -dimensional unit sphere. The above invariance principle yields $\Theta_2 \approx 1.26$ ⁶¹ and $\Theta_3 \approx 0.23$ ⁵⁴. Comparison with other percolation criteria, in particular in the Mott regime^{36,62,63}, indicate that in $2D$ a slightly smaller value $\Theta_2 \approx 1$ yields results closer to the numerically found percolation threshold. In the main part of the paper we therefore used the latter value.

To implement the percolation criterion for an arbitrary density of states, as obtained after the sudden application of a gate voltage, it is convenient to introduce the functions

$$F_{ph}(E) = 2 \int_0^E d\epsilon \rho(\epsilon) \rho(\epsilon - E) \quad (\text{A5})$$

$$F_{pp}(E) = \rho(E) \int_0^E d\epsilon \rho(\epsilon) \quad (\text{A6})$$

$$F_{hh}(E) = \rho(-E) \int_{-E}^0 d\epsilon \rho(\epsilon) \quad (\text{A7})$$

and $\Phi_{\alpha\beta}(E) = \int_0^E d\epsilon F_{\alpha\beta}(\epsilon)$ with $\alpha, \beta \in \{p, h\}$, in terms

of which the percolation criterion (A4) can be rewritten as

$$\Theta_D = \int_0^{\xi\chi_c/2} d^D r V_D \left(\frac{r}{2}\right)^D \cdot \quad (\text{A8})$$

$$[\Phi_{pp}(T(\chi_c - 2r/\xi)) + \Phi_{hh}(T(\chi_c - 2r/\xi)) + \Phi_{ph}(T(\chi_c - 2r/\xi) + e^2/\kappa r) - \Phi_{ph}(e^2/\kappa r)].$$

For completeness we report the standard expressions that one obtains in the limiting case of a constant density of states ($\rho(\epsilon) \equiv \nu_0$) and high temperatures ($T \ll T_X$, Mott regime), and in presence of Efros-Shklovskii pseudogap, $\rho(\epsilon) = \alpha_D(\kappa/e^2)^D \epsilon^{D-1}$, ($T < T_X$). In these cases the above criterion is readily evaluated analytically and yields the threshold values

$$\chi_c = \left(\frac{T_M^D}{T}\right)^{1/(D+1)}, \quad (\text{Mott}) \quad (\text{A9})$$

$$\chi_c = \left(\frac{T_{ES}^D}{T}\right)^{1/2}, \quad (\text{Efros-Shklovskii}) \quad (\text{A10})$$

with

$$T_M^{(D)} = \frac{C_M^{(D)}}{\nu_0 \xi^D} \quad (\text{A11})$$

$$T_{ES}^{(D)} = C_{ES}^{(D)} \frac{e^2}{\kappa \xi} \quad (\text{A12})$$

The numerical constants $C_M^{(D)}$ depend on the value of Θ_D , while $C_{ES}^{(D)}$ varies with the value of Θ_D/α_D^2 . In the main text we used $\Theta_2 = 1$, for which one finds $C_M^{(2)} \approx 13.9$. (Using $\Theta_3 = 0.23$ ⁵⁴, one obtains $C_M^{(3)} \approx 19.4$). With $\alpha_D = D/\pi$, as suggested by Efros' self-consistency argument³⁹, one further finds $C_{ES}^{(2)} \approx 5.6$ ⁶¹ and $C_{ES}^{(3)} \approx 2.6$ ⁵⁴.

-
- ¹ J. Davies, P. Lee, and T. Rice, Phys. Rev. Lett. **49**, 758 (1982).
² M. Grünwald, B. Pohlmann, L. Schweitzer, and D. Würtz, J. Phys. C **15**, L1153 (1982).
³ J. Davies, P. Lee, and T. Rice, Phys. Rev. B **29**, 4260 (1984).
⁴ M. Pollak, Philos. Mag. B **50**, 265 (1984).
⁵ D. Monroe *et al.*, Phys. Rev. Lett. **59**, 1148 (1987).
⁶ M. Ben-Chorin, Z. Ovadyahu, and M. Pollak, Phys. Rev. B **48**, 15025 (1993).
⁷ A. Vaknin, Z. Ovadyahu, and M. Pollak, Phys. Rev. Lett. **81**, 669 (1998).
⁸ A. Vaknin, Z. Ovadyahu, and M. Pollak, Phys. Rev. Lett. **84**, 3402 (2000).
⁹ V. Orlyanchik and Z. Ovadyahu, Phys. Rev. Lett. **92**, 066801 (2004).
¹⁰ Z. Ovadyahu, Philos. Mag. B-Phys. Condens. Matter Stat. Mech. Electron. Opt. Magn. Prop. **81**, 1225 (2001).
¹¹ Z. Ovadyahu and M. Pollak, Phys. Rev. B **68**, 184204 (2003).
¹² A. Vaknin, Z. Ovadyahu, and M. Pollak, Phys. Rev. B **65**, 134208 (2002).
¹³ C. Adkins *et al.*, J. Phys. C **17**, 4633 (1984).
¹⁴ T. Grenet, Eur. Phys. J. B **32**, 275 (2003).
¹⁵ G. Martinez-Arizala *et al.*, Phys. Rev. Lett. **78**, 1130 (1997).
¹⁶ G. Martinez-Arizala *et al.*, Phys. Rev. B **57**, R670 (1998).
¹⁷ T. Grenet, phys. stat. sol. (c) **1**, 9 (2004).
¹⁸ A. Vaknin, Z. Ovadyahu, and M. Pollak, Europhys. Lett. **42**, 307 (1998).
¹⁹ M. Pollak, Disc. Faraday Soc. **50**, 13 (1970).
²⁰ A. L. Efros and B. I. Shklovskii, J. Phys. C **8**, L49 (1974).

- ²¹ M. Müller and L. B. Ioffe, Phys. Rev. Lett. **93**, 256403 (2004).
- ²² S. Pankov and V. Dobrosavljević, Phys. Rev. Lett. **94**, 046402 (2005).
- ²³ A. Zabrodskii, Philos. Mag. B-Phys. Condens. Matter Stat. Mech. Electron. Opt. Magn. Prop. **81**, 1131 (2001).
- ²⁴ J. Massey and M. Lee, Phys. Rev. Lett. **75**, 4266 (1995).
- ²⁵ W. Teizer, F. Hellman, and R. Dynes, Phys. Rev. Lett. **85**, 848 (2000).
- ²⁶ B. Sandow *et al.*, Phys. Rev. Lett. **86**, 1845 (2001).
- ²⁷ V. Butko, J. DiTusa, and P. Adams, Phys. Rev. Lett. **84**, 1543 (2000).
- ²⁸ M. Lee, J. Massey, V. Nguyen, and B. Shklovskii, Phys. Rev. B **60**, 1582 (1999).
- ²⁹ S. D. Baranovskii, B. I. Shklovskii, and A. L. Efros, Sov. Phys. JETP **60**, 1031 (1984).
- ³⁰ J. P. Bouchaud, J. Phys. I France **2**, 1705 (1992).
- ³¹ A. Vaknin, Z. Ovadyahu, and M. Pollak, Phys. Rev. B **61**, 6692 (2000).
- ³² C. Yu, Phys. Rev. Lett. **82**, 4074 (1999).
- ³³ D. Tsigankov, E. Pazy, B. Laikhtman, and A. Efros, Phys. Rev. B **68**, 184205 (2003).
- ³⁴ V. Orlyanchik, A. Vaknin, Z. Ovadyahu, and M. Pollak, phys. stat. sol. b **230**, 61 (2002).
- ³⁵ A. Efros and B. Shklovskii, in *Electron-Electron interaction in disordered systems*, edited by A. Efros and M. Pollak (North-Holland, Amsterdam, 1985).
- ³⁶ B. Shklovskii and A.L.Efros, *Electronic properties of doped semiconductors* (Springer, Heidelberg, 1984).
- ³⁷ Z. Ovadyahu, Phys. Rev. B **47**, 6161 (1993).
- ³⁸ O. Cohen and Z. Ovadyahu, Phys. Rev. B **50**, 10442 (1994).
- ³⁹ A. L. Efros, J. Phys. C **9**, 2021 (1976).
- ⁴⁰ E. R. Grannan and C. C. Yu, Phys. Rev. Lett. **71**, 3335 (1993).
- ⁴¹ T. Vojta and M. Schreiber, Phys. Rev. Lett. **73**, 2933 (1994).
- ⁴² E. Grannan and C. Yu, Phys. Rev. Lett. **73**, 2934 (1994).
- ⁴³ A. I. Larkin and D. E. Khmel'nitski, Sov. Phys. JETP **56**, 647 (1982).
- ⁴⁴ N. Markovic *et al.*, Phys. Rev. B **62**, 2195 (2000).
- ⁴⁵ M. Overlin, L. Wong, and C. Yu, Phys. Rev. B **70**, 214203 (2004).
- ⁴⁶ D. Menashe, O. Biham, B. Laikhtman, and A. Efros, Europhys. Lett. **52**, 94 (2000).
- ⁴⁷ D. Grempel, Europhys. Lett. **66**, 854 (2004).
- ⁴⁸ Z. Ovadyahu, private communication.
- ⁴⁹ A. Perez-Garrido, M. Ortuno, A. Diaz-Sanchez, and E. Cuevas, Phys. Rev. B **59**, 5328 (1999).
- ⁵⁰ D. Menashe, O. Biham, B. Laikhtman, and A. Efros, Phys. Rev. B **64**, 115209 (2001).
- ⁵¹ A. B. Kolton, D. R. Grempel, and D. Dominguez, Phys. Rev. B **71**, 024206 (2005).
- ⁵² V. Ambegaokar, B. I. Halperin, and J. S. Langer, Phys. Rev. B **4**, 2612 (1971).
- ⁵³ M. Pollak, J. Non-Cryst. Solids **11**, 1 (1972).
- ⁵⁴ A. L. Efros, V. L. Nguyen, and B. I. Shklovskii, Solid State Commun. **32**, 851 (1979).
- ⁵⁵ A. Aharony, Y. Zhang, and M. P. Sarachik, Phys. Rev. Lett. **68**, 3900 (1992).
- ⁵⁶ Y. Meir, Phys. Rev. Lett. **77**, 5265 (1996).
- ⁵⁷ R. Rosenbaum, Phys. Rev. B **44**, 3599 (1991).
- ⁵⁸ Taking the conservative estimate $\alpha_2 = 2/\pi$, the glass transition T_g in strongly disordered 2D systems is expected to be larger than E_C by a numerical factor of approximately 5 (see Eq. (13)). It may be even larger, taking into account that the relevant α_2 for quasiparticle excitations is probably larger than the Efros-Shklovskii prediction.
- ⁵⁹ M. Sarvestani, M. Schreiber, and T. Vojta, Phys. Rev. B **52**, R3820 (1995).
- ⁶⁰ M. Pollak and M. Ortuno, in *Electron-electron interaction in disordered systems*, edited by A. Efros and M. Pollak (North-Holland, Amsterdam, 1985).
- ⁶¹ V. L. Nguyen, Sov. Phys. Semicond. **18**, 207 (1984).
- ⁶² C. H. Seager and G. E. Pike, Phys. Rev. B 1435 (1974).
- ⁶³ G. E. Pike and C. H. Seager, Phys. Rev. B 1421 (1974).